In-situ transport and microstructural evolution in GaN Schottky diodes and epilayers exposed to swift heavy ion irradiation

Ashish Kumar,[1,a)] R. Singh,[2] Parmod Kumar,[1] Udai B. Singh,[1] K. Asokan,[1] Platon A. Karaseov,[3] Andrei I. Titov,[3] and D. Kanjilal[1]
[1]*Inter-University Accelerator Centre, Aruna Asaf Ali Marg, Vasant Kunj, New Delhi 110067, India*
[2]*Department of Physics, Indian Institute of Technology Delhi, Hauz Khas, New Delhi 110016, India*
[3]*Department of Physical Electronics, Peter the Great St. Petersburg Polytechnic University, Polytechnicheskaya st., 29, Saint Petersburg, Russia*

(Received 12 July 2017; accepted 28 October 2017; published online 5 December 2017)

A systematic investigation of radiation hardness of Schottky barrier diodes and GaN epitaxial layers is carried out by employing *in-situ* electrical resistivity and cross sectional transmission electron microscopy (XTEM) microstructure measurements. The change in the current transport mechanism of Au/n-GaN Schottky barrier diodes due to irradiation is reported. The role of irradiation temperature and ion type was also investigated. Creation of damage is studied in low and medium electron energy loss regimes by selecting different ions, Ag (200 MeV) and O (100 MeV) at various fluences at two irradiation temperatures (80 K and 300 K). GaN resistivity increases up to 6 orders of magnitude under heavy Ag ions. Light O ion irradiation has a much lower influence on sheet resistance. The presence of isolated defect clusters in irradiated GaN epilayers is evident in XTEM investigation which is explained on the basis of the thermal spike model. *Published by AIP Publishing.* https://doi.org/10.1063/1.4995491

INTRODUCTION

GaN-based electronic and optoelectronic devices have witnessed significant progress in technology. GaN has high radiation hardness that makes it a material of interest for applications such as space satellites, avionics, and detectors, where electronic systems are exposed to fluxes of protons, α-particles, heavier ions from solar flares, electrons, and γ-rays or cosmic rays. GaN based devices have better stability and reliability (attributed to strong Ga-N bonding) as compared to Si and GaAs as remarkable degradation in GaN starts at about two orders of higher magnitude of radiation fluences.[1,2] A low earth orbit extends up to ∼1000 km from the surface of Earth, and energetic particles with energies up to hundreds of MeV, such as electrons, protons, and heavy ions, have been trapped at these heights.[3] These particles will strongly affect properties and operation of an electronic device mounted on a satellite.

Ion-induced effects in this material have certainly been studied by a number of various groups. However, most of the earlier investigations were done in the keV regime,[4] while there are very few studies available in the swift heavy ion (SHI) regime.[5–9] In the case of the keV heavy ion impact, nuclear (elastic) energy loss (S_n) is more dominant than energy loss due to ionization and electronic excitations [electronic energy loss (S_e)]. For light ion irradiation in the same keV regime, electronic loss is more prononced, but its magnitude is still not too high. In the case of swift heavy ions with energy ∼100 MeV, the electronic loss is giant and much higher than the nuclear one. For example, the 200 MeV Ag ion penetrating in GaN has S_e (∼25.94 keV/nm) which is three orders of magnitude higher than S_n (∼0.07 keV/nm) as calculated by SRIM-2008.[10] Less energetic light O ions (100 MeV) have an order of magnitude lower value of electronic loss, whereas the S_e/S_n ratio is an order higher than that for the Ag beam (see Table I).

It can be argued that kinds of defects in keV and MeV regimes will be formed by significantly different mechanisms. Indeed, it is well established that light ion irradiation of GaN with an energy of ≤1 MeV mainly forms point defect clusters.[4,11] SHI irradiation may lead to the creation of relatively big 3-dimentional damaged areas known as ion tracks.[12] Hence, the formation of electrically isolative layers under ion bombardment can go significantly different ways in these regimes and is driven by different mechanisms.

In addition, for electronic devices like Schottky barrier diodes (SBDs), SHI reaches deep inside the bulk, which is different from the low-energy ion implantation where the ions are implanted in the depletion region near the Schottky interface. In this way, SHI beam irradiation can be used as a tool to modify metal - semiconductor (M–S) interface in a controlled manner either by creating specific types of defects at the interface or by annealing the already existing defects,[3] without leaving any implanted ions near the depletion region.

The lack of experimental data in the SHI energy regime for a strategic material like GaN at different temperatures (80 K and 300 K) makes it difficult to develop a proper model for defect and other property evolution mechanisms. Thus, the aim of the present investigation is to study the change in electrical properties of epitaxial n-GaN layers irradiated with relatively light (O) and heavy (Ag) ions at different temperatures (80 K and 300 K). In addition, ion-beam-induced change in I–V characteristics of Schottky surface barrier diodes will be studied. For example, irradiation of

[a)]Electronic addresses: ashish@iuac.res.in and dr.akmr@gmail.com

TABLE I. Experimental parameters and calculated values of electronic (S_e) and nuclear (S_n) energy loss for Ag and O ion beams in GaN.

Ions	Ag	O
Energy (MeV)	200	100
S_e (keV/nm)	25.94	1.476
S_n (keV/nm)	7.11×10^{-2}	8.358×10^{-4}
S_e/S_n	365	1766
Vacancies/ion	705.5	9.5
Irradiation temperature (K)	300 and 80	300 and 80

GaN epitaxial layers and SBDs by 200 MeV Ag ions at fluencies used in the present study is equivalent to a few decades exposure in low earth orbit.[3] Therefore, this work is important for understanding the ion–solid interaction mechanisms necessary for designing technologically improved and radiation hard electronics. Experiments were also planned to investigate not only the effect of irradiation temperature on the defect cascade mechanism but the effect of *in-situ* vs. *ex-situ* measurements (room temperature defect annealing/evolution with time).

EXPERIMENTAL

Un-intentionally doped ($N_d^+ \sim 3 \times 10^{16}\,cm^{-3}$) GaN epitaxial layers (~3.7 μm thick) grown by the metal-organic chemical vapour deposition technique on the sapphire substrate were used for SHI irradiation with 200 MeV $^{107}Ag^{14+}$ and 100 MeV $^{16}O^{7+}$ over a wide fluence range at two irradiation temperatures (80 K and 300 K) using the 15 MV Pelletron facility at the Inter-University Accelerator Center, New Delhi.[5,6,13] The pristine sample resistivity for GaN epitaxial layers was ~8 Ω cm and ~5 Ω cm at 300 K and 80 K, respectively. This difference came from variation in concentration and sample geometry, as the samples were research grade. For *in-situ* resistivity measurements (van der-Pauw method), electrical connections to the sample contact pads were taken out from the irradiation chamber to an Agilent Semiconductor Analyzer (B1500A). A standard protocol was employed where the electrical measurements were performed within 10 min after application of each ion fluence step. For *ex-situ* measurements, samples were irradiated at different fluences first and then electrical measurements were performed in lab after taking out the samples from the irradiation chamber. The "Normal" *flux effect* was minimized by maintaining the same flux value (6.25×10^9 ions $cm^{-2}s^{-1}$) for all irradiation experiments.[14] The microstructure investigation of GaN samples was carried out using cross sectional transmission electron microscopy (XTEM) performed by an FEI TITAN 80–300 machine. Prior to irradiation, epitaxial films were sequentially (i) cleaned with methyl propanol for 8 min at around 80 °C, (ii) dipped in acetone for 7 min at 50 °C, (iii) cleaned with iso-propanol for 3 min in an ultrasonic bath, and again (iv) rinsed with deionized water and blown with N_2 for drying the sample. For lithography/lift-off techniques, a photoresist (AZ5214), developer (AZ 400k: H_2O 1:4), and native oxide layer removal (50% HCl for 60 s, rinse in H_2O) were used in a Class 100 clean room facility as explained in previous studies.[13] All Au/n-GaN diodes (100 nm thick Au contact) were fabricated by the e-beam deposition system in ultra-high vacuum (UHV) with varying diameters (4–384 μm), and thick indium ohmic contacts were deposited in the second step.

RESULTS AND DISCUSSION

A Monte-Carlo simulation (SRIM/TRIM-2008) of 200 MeV ^{107}Ag and 100 MeV O ions in GaN was carried out, and the results are given in Table I. It can be seen that magnitudes of electronic (S_e) and nuclear (S_n) energy loss for the Ag ion are higher than those for the O ion in GaN, which results in more vacancies/ion for the Ag ion. The energy loss for the 200 MeV Ag ion in the Au/n-GaN/Sapphire (100 nm/3.7 μm/300 μm) Schottky diode structure is shown in Fig. 1. The range of 200 MeV Ag ions in the device structure is ~20 μm which is deep in the sapphire substrate. Therefore, no Ag ions will be implanted at the Au/n-GaN interface of the diode. It is clearly seen that S_e is dominant at the Au–GaN interface. In fact, it is three orders higher than the S_n.

Figure 2 shows the *I–V* characteristics of pristine and post-irradiated SBDs (200 MeV $^{107}Ag^{14+}$ ions at different fluences) measured at 300 K. For each fluence, at least ten diodes with almost identical electrical characteristics are analyzed and an average behavior is shown here for each set. It is clearly seen that irradiation affects the *I-V* characteristics of Au/n-GaN SBDs.

For calculations of electrical parameters of Schottky diodes, thermionic emission equations are used[16]

$$I = I_O \exp\left(\frac{q[V - IR_{SR}]}{nkT}\right), \tag{1}$$

$$I_O = AA^{**}T^2 \exp\left(\frac{-q[\phi_b - \Delta\phi_b]}{kT}\right), \tag{2}$$

$$n = \frac{q}{kT\left(\frac{dV}{d\ln I}\right)}. \tag{3}$$

Here, symbol ϕ_b represents the barrier height, $\Delta\phi_b$ is the image force barrier lowering, n is the ideality factor, I_o is the reverse saturation current, R_{SR} is the series resistance, A is the diode area, A^{**} is the Richardson constant (for GaN 26.4 A $cm^{-2}K^{-2}$), and other symbols have their usual

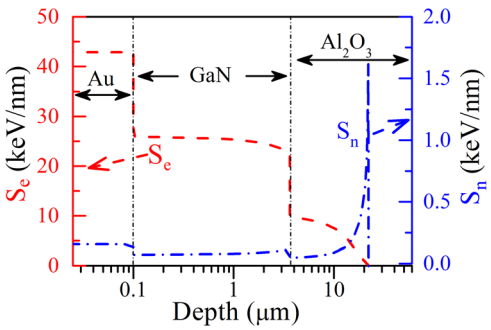

FIG. 1. Calculated values of electronic (S_e) and nuclear (S_n) energy loss for 200 MeV $^{107}Ag^{14+}$ ions in the Au/n-GaN/Sapphire (100 nm/3.7 μm/300 μm) Schottky diode structure from SRIM–2008.

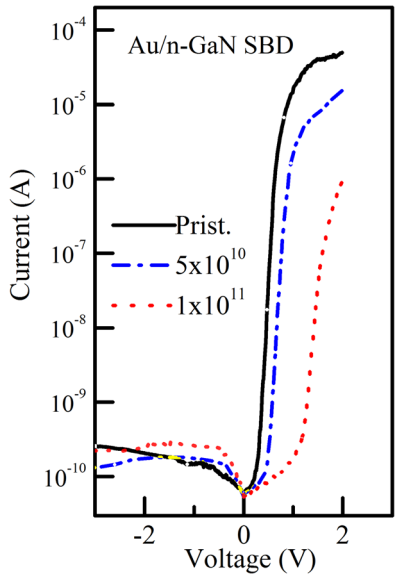

FIG. 2. I-V characteristics of Au/n-GaN SBDs exposed to 200 MeV $^{107}Ag^{14+}$ ions at different fluences. A constant beam flux of $6.25 \times 10^9\,cm^{-2}s^{-1}$ at 300 K was used.

meanings. The Schottky barrier height (SBH) and ideality factor calculated from the intercept and slope of forward *log I* vs. *V* characteristics[5,6] are listed in Table II. The series resistance for pristine and irradiated diodes is calculated using the Cheung and Cheung method.[15] It can be observed that both the barrier height and the ideality factor increase with fluence. A similar study by Baranwal *et al.*[17] for the Au/GaN Schottky diode has shown that the barrier height increases for low fluences and then decreases with a further increase in fluence. They attributed this enhancement in the barrier height to increased state density at the Au-GaN interface induced by ion energy loss processes and approaching of the Bardeen limit for the Schottky barrier. In 130 MeV Au^{12+} ion irradiated Au/n-Si Schottky diodes, Kumar *et al.*[18] have reported that the presence of high recombination current due to irradiation caused the defect concentration. Our previous investigations with the Ni/GaN diode also have a similar trend in the barrier height where it was found that image force lowering $\Delta\phi_b$ plays an important role in pristine as well as irradiated diodes.[5,6]

It should be noted here that the increase in the Schottky barrier height may appear due to decreased carrier concentrations (and hence lower magnitude of $\Delta\phi_b$). The nature of the Schottky metal (work function, alloying)[19] may also affect the interface. The presence of defects at the metal-semiconductor interface induces the current transport mechanism other than thermionic emission, which is evident from

TABLE II. Diode parameters for Au/n-GaN SBDs calculated from thermionic emission equations.

Fluence (ions/cm^2)	Ideality factor (n)	ϕ_b (eV)	Rev. Leak. Curr. I_R at –1 V (nA)	Series resistance (Ω) by Cheung's method[15]
Pristine	1.4	0.85	15	1.5 k
5×10^{10}	1.8	0.99	18	5.2 k
1×10^{11}	2.4	1.16	26	3.4 M

the increased ideality factor at higher fluences (1.8 for 5×10^{10} ions cm^{-2} and 2.4 for 1×10^{11} ions cm^{-2} as compared to 1.4 for pristine diodes).

In order to study the SHI irradiation induced carrier concentration decrease, we performed *in-situ* investigation of GaN epitaxial film resistivity. Figure 3(a) shows the normalized resistivity R_S (irradiated sample resistivity divided by pristine sample resistivity) of GaN samples irradiated with 200 MeV Ag and 100 MeV O ions at two temperatures 80 K and 300 K using a constant beam current (also see supplementary material). A general increase in R_S is observed with higher ion fluences as shown in Fig. 3(a). The normalized resistivity in GaN rose sharply for the Ag beam as compared to the O ion beam. It can be attributed to the creation of more damage by heavy Ag ions compared to lighter O ions (Table I) that act as charge trap centers or scattering centers.[20] It is evident from Fig. 1(a) that the electrical isolation process in GaN is weakly affected by the irradiation temperature. Indeed, the ion fluence required to achieve a given magnitude of normalized resistivity slightly increases with irradiation temperature. However, this can be caused by different initial sample resistances. Further work is needed to clarify this question.

It is obvious that R_s behaviour evidenced in Fig. 3(a) is related to the trapping of charge carriers by irradiation-produced deep centres and the decrease in charge carrier mobility.[5,6,14] The exact nature of trap centres is not well understood yet. Look *et al.*[21] have first reported that N interstitials in GaN can act as acceptor defects that are generated by high energy (0.7–1.0 MeV) electron irradiation. However, subsequent reports suggested the presence of Frenkel pairs and various other complex defects that act as charge traps for electrons, and hence, the *resist*ivity increases.[22] Investigations by Kucheyev *et al.*[14] have established the role of efficient dynamic annealing in GaN at 80 K and higher temperatures. Although most of the ion beam created Frenkel pairs are annealed during short time span, dynamic annealing is imperfect which leads to lattice damage accumulation with further increasing ion fluence. As a result, in the keV regime, the stable damage is controlled by irradiation temperature, the density of collision cascades (which in turn depends on incident ion energy and mass), and the beam flux.

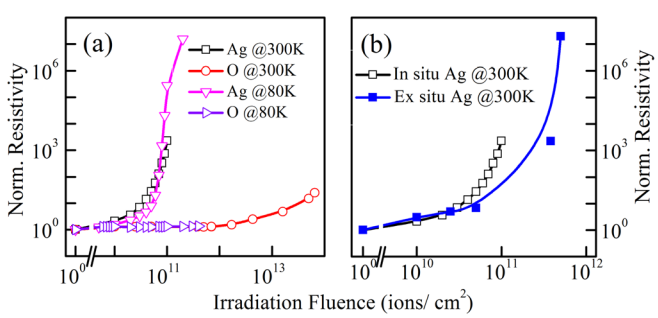

FIG. 3. Fluence dependence of normalized resistivity of GaN with 200 MeV Ag ions and 100 MeV O ions with a constant beam flux of $6.25 \times 10^9\,cm^{-2}s^{-1}$ at different temperatures (a), as indicated in the legend. Panel (b) presents the comparison of *ex-situ* and *in-situ* measurements for the Ag ion at 300 K.

TABLE III. GaN thermodynamic parameters used in the calculation.

ρ_S (g/cm^3)	ρ_L (g/cm^3)	T_m (K)	T_V (K)	Q_m (J/g)	Q_V (J/g)	λ (nm)	Therm. Cond. (W cm^{-1}°K^{-1})	Specific Heat (J g^{-1}°K^{-1})
6.15 (Ref. 30)	6.15 (Ref. 30)	2773 (Ref. 31)	$\sim 10^4$	1599.05 (Ref. 30)	8644.84 (Ref. 30)	5.0 (Ref. 29)	$\sim$10.4 (80 K) (Ref. 32) 1.3 (300 K) (Ref. 33)	40.8 (300 K) (Ref. 29) 0.49 (80 K) (Ref. 34)

Figure 3(b) depicts the evolution of R_S of GaN samples irradiated by 200 MeV Ag ions at 300 K in *ex-situ* (solid symbol) and *in-situ* (open symbol) measurements, respectively. The *in-situ* resistivity was found to be increasing at a higher rate compared to *ex-situ* resistivity for the same fluences. This is correlated with pronounced long-term annihilation of defects formed in GaN during SHI irradiation which are prompted on the experimental time scale, and hence, the electrical resistance decreases after some time. Indeed, the level of dynamic annealing is controlled by the effective diffusivity of irradiation generated defects, which is related to various processes, e.g., trapping and de-trapping of migrating defects, defect density in the lattice, chemical potential position, and radiation supported migration. Similar results were reported by Coskun *et al.*[23] in *n-type* ZnO irradiated with 1.0 and 1.5 MeV electrons at 130 K where such behaviour was associated with rapid defect annihilations (<1 min). Kucheyev *et al.*[14] also showed that electrical isolation vanished for light ^{1}H ions (0.6 MeV), which was attributed to the perfect dynamic annealing of point defects in very dilute collision cascades at 80 K temperature. Therefore, the study of dynamic annealing at low ion fluences of SHI irradiation (for electric isolation purpose) is important in view of irradiation-temperature and beam-cascade.

Furthermore, SHI irradiation causes the formation of different stable complex defects some of which can be detected and imaged by TEM as defect clusters or extended defects.

The possibility of latent track formation is correlated with the energy deposited in electronic excitation processes. Lattice behavior in this case is described with the help of the thermal spike model given by Toulemonde *et al.*[24,25] This model quantitatively describes the track formation in the inelastic collision energy regime for insulators[26,27] and metals[25,28] by calculating the energy transfer from an incident ion to target electrons and lattice atoms. The mathematical formulation is given by two coupled differential equations relating temporal (t) and spatial (r) energy transfer in atomic and electronic subsystems[24,25]

$$C_e(T_e)\frac{\partial T_e}{\partial t}=\frac{1}{r}\frac{\partial}{\partial r}\left[rK_e(T_e)\frac{\partial T_e}{\partial r}\right]-g(T_e-T_a)+A(r,t), \quad (4)$$

$$C_a(T_a)\frac{\partial T_a}{\partial t}=\frac{1}{r}\frac{\partial}{\partial r}\left[rK_a(T_a)\frac{\partial T_a}{\partial r}\right]+g(T_e-T_a), \quad (5)$$

where indices e and a represent the electronic and lattice subsystems. Symbol C is the specific heat coefficient, T is the temperature, and K represents the thermal conductivity. A numerical solution of these equations provides information of all the parameters as a function of temperature. The deposited or transferred energy into the target is assumed to correspond to electronic energy loss when the initial energy distribution of the electrons $A(r,t)$ is integrated over space and time. The electron–phonon coupling coefficient g is related to the mean free path λ (Ref. 29) and represents the transfer of heat from the electronic subsystem to the lattice subsystem. All the parameter values for GaN were taken from the literature as listed in Table III along with corresponding references used. Figures 5(a)–5(d) present the results of thermal spike calculations using $\lambda = 5$ nm.[29] The lattice temperature is plotted as a function of space and time parameter.

It is observed that the lattice temperature overcomes the melting temperature of GaN ($\sim$2773 K)[31] for the 200 MeV Ag ion beam for both irradiation temperatures (300 K and 80 K). The local melting may occur along the ion trajectory that produces a permanent phase transformation for the Ag ion beam. Quenching of molten tracks leads to the incomplete recrystallization of highly disordered regions, creating complex defects, point defects, and clusters in the material. The lattice temperature was achieved high enough to form a track with a diameter of $\sim$6 nm for the Ag ion beam at 300 K irradiation and 80 K [Figs. 4(a) and 4(c)]. For the O ion, the maximum lattice temperature was much below melting temperature for both cases [Figs. 4(b) and 4(d)]. Smaller complex defects may also form when point defects (native or created by ions beam) combine or mix with the ion track core before it is completely cooled.[6]

Figure 5 shows bright field cross-sectional TEM (XTEM) images of epitaxial GaN samples taken in the (g = 0002*) direction. The surfaces of the layers appear to be flat as shown for all samples. This is consistent with the high-resolution TEM image analysis studied in Refs. 5, 6,

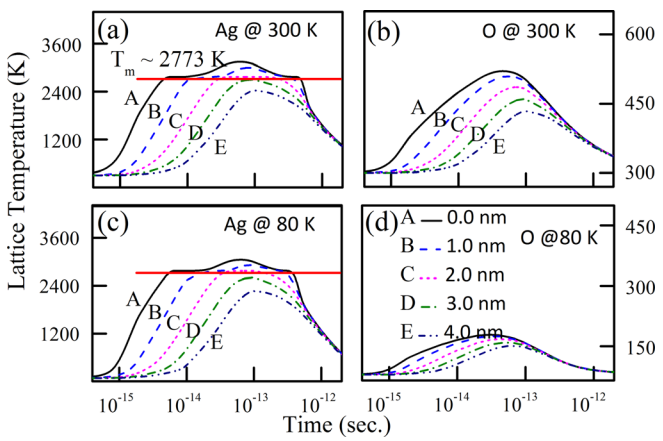

FIG. 4. Evolution of lattice temperature of GaN as a function of time at different radial distances from ion path/trajectory for (a) 200 MeV Ag ion at 300 K, (b) 100 MeV O ion at 300 K, (c) 200 MeV Ag ion at 80 K, and (d) with 100 MeV O ions at 80 K, as indicated in the legend. The melting temperature (T_m) for GaN is 2773 K.

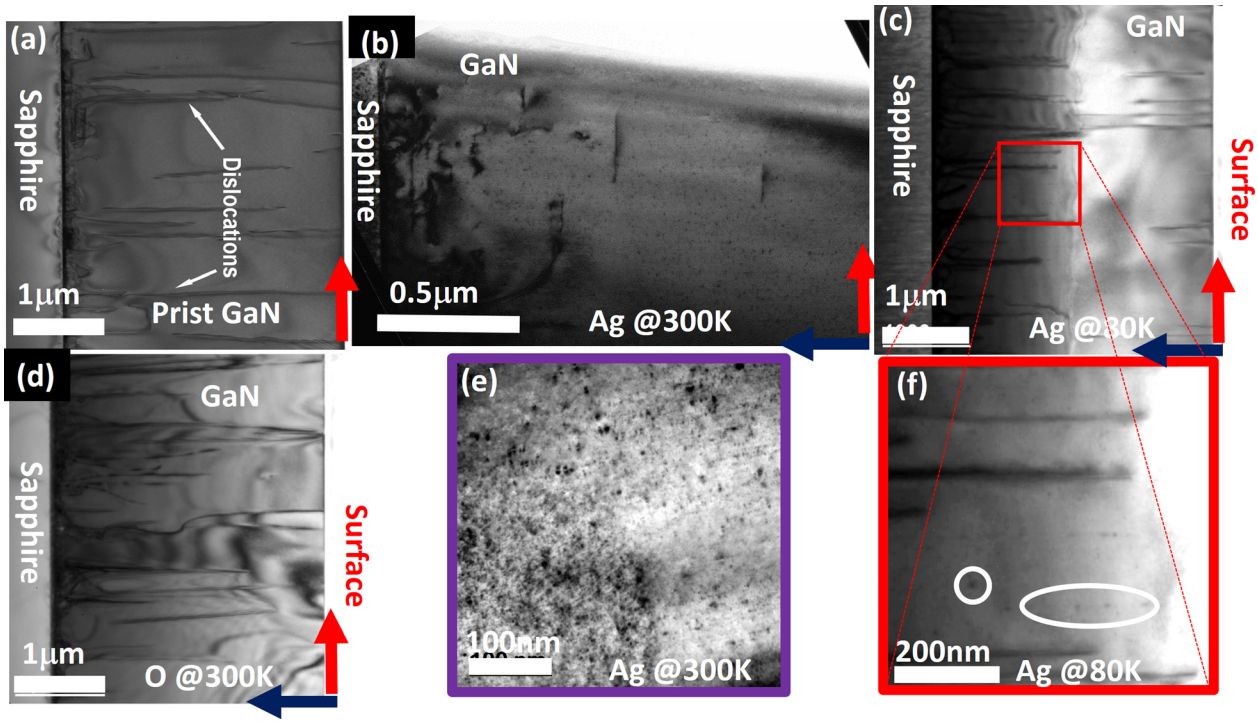

FIG. 5. Bright field XTEM image (g = 0002*) of (a) pristine GaN, irradiated with (b) 200 MeV Ag ions to a fluence of 5×10^{12} ions cm^{-2} at 300 K, (c) 200 MeV Ag ions to a fluence of 5×10^{11} ions cm^{-2} at 80 K, and (d) 100 MeV O ions to a fluence of 5×10^{12} ions cm^{-2} at 300 K. (e) and (f) show higher magnification images of (b) and (c), respectively. Circles in (f) show the aligned chain of defect clusters formed by 200 MeV Ag ions.

and 9 which showed the absence of amorphization on the surface and bulk, which were visibly crystalline in the image. The EDX analysis of these regions (not shown here) showed the presence of only Ga and N, thus excluding other possibilities of creation of defects (native, impurities) compared to that caused by irradiation.[5] The presence of threading dislocations (originating from the GaN/sapphire interface) is clearly seen in all these samples including the pristine GaN [Fig. 5(a)]. It is also seen that in accordance with thermal spike calculations, O ion irradiation (causes mainly point defects) does not form any big defect complex visible in XTEM images [Fig. 5(d)]. On the other hand, a number of isolated defect clusters of sizes 2–20 nm were formed in epilayers irradiated with Ag ions at 300 K as can be seen in Fig. 5(b). These defects most probably correspond to defect clusters, dislocation loops, and dipoles (vacancy loops).[35,36] Similar defects are also formed at low temperature (80 K) irradiation of Ag ions but with much less density compared with the 300 K irradiated sample [see Fig. 5(c)]. In the samples irradiated at 80 K, disordered regions are lined up along the beam path in the target [Figs. 5(c) and 5(f)]. Figures 5(e) and 5(f) present magnified images of these defect cluster areas appearing in the Ag-irradiated samples. To our opinion, the difference in defect cluster density in Figs. 5(e) and 5(f) is due to the temperature difference and lower fluence used to irradiate the sample in Figs. 5(c) and 5(f). Indeed, on the one hand, it can be estimated that to cover the sample surface with overlapping 10-nm-diameter tracks, a critical irradiation fluence of 1×10^{12} ions cm^{-2} is needed. At higher fluences, defect overlapping starts, resulting in the formation of defect clusters. For example, in GaN irradiated with 132 MeV $^{209}Pb^{32+}$ at 300 K, circular ion impacts of diameter 8 nm were formed at irradiation fluences of 5×10^{10} ions cm^{-2}.[7] Two concentric regions around the ion path were observed; the inner region corresponds to the section of the ion path where the lattice temperature crosses the melting temperature of GaN and an outer strained region where the melting temperature was not attained. For 930 MeV ^{208}Pb ions, amorphous continuous tracks were formed at a fluence of 2×10^{11} ions cm^{-2}.[8] Similarly, the formation of near-continuous latent tracks of diameter 10 nm was also observed in GaN irradiated with 200 MeV Au ions at a fluence of 2×10^{11} ions cm^{-2}.[20] On the other hand, at higher temperature, defect clusters might be larger since the energy spike dissemination depends not only on energy and mass of the incident ion but on target temperature as indicated by model calculations [see Figs. 4(a) and 4(c)]. Hence, critical fluence needed for defect overlapping must be lower at high temperature and damage will form clusters effectively.

Therefore, the results obtained from XTEM images are in good agreement with the thermal spike calculations which predict disordered regions and defect clusters along the ion track core in Ag irradiated GaN due to the high local lattice temperature. These defect clusters can act as effective traps decreasing the carrier concentration and mobility. However, the temperature difference found in damaged area formation efficiency does not directly correlate with the very slight temperature difference in the behaviour of GaN sheet resistance. Thus, indeed, spike-induced defect clusters play a role in carrier dynamics, but other mechanisms might also be important. More experimental data in SHI irradiation are needed to identify the exact origin of defect generation and mechanisms of electrical degradation in GaN. The present

investigation is one such systematic approach for studying the effect of two irradiation parameters (i.e., ion type and irradiation temperature) on the electrical and microstructural properties of GaN in the SHI energy regime.

CONCLUSIONS

SBDs irradiated by 200 MeV Ag ions at 300 K show that heavy ion irradiation affects the electrical transport mechanisms at the interface by introducing electrically active defects. The role of the kind of ion and irradiation temperature in the evolution of defects in GaN has been investigated using *in-situ* resistivity and XTEM techniques. The normalized resistivity rose sharply for Ag ions and very slightly for light O ions. The lattice damage or disorder depends on the magnitude of defect cascades which is largely governed by incident ion mass and energy. The permanent damage in GaN is limited by defect annihilation that is rapid on the experimental time scale and electrical isolation degrades after some time as depicted by *in-situ* and *ex-situ* resistivity measurements. Thermal spike calculations suggest that for heavier Ag ions, larger energy deposited to the target lattice results in locally molten regions along the ion path. This leads to the formation of defect cluster chains that are visible in XTEM images. Spike-induced defect clusters play a role in carrier dynamics and irradiation-induced degradation, but other mechanisms might also be important.

SUPPLEMENTARY MATERIAL

See supplementary material for raw data of Fig. 3, i.e., fluence dependence of resistivity of GaN with 200 MeV Ag ions and 100 MeV O ions at different temperatures.

ACKNOWLEDGMENTS

A.K. would like to acknowledge the financial support received from the Department of Science and Technology, India through DST-INSPIRE Faculty scheme (DST/INSPIRE/04/2015/001572). Technical support from Dr. A. Hähnel from the Max-Planck Institute of Microstructure Physics, Halle, Germany is also acknowledged.

[1]S. J. Pearton, R. Deist, F. Ren, L. Liu, A. Y. Polyakov, and J. Kim, J. Vac. Sci. Technol. A: Vac., Surf., Films **31**, 050801 (2013).
[2]S. J. Pearton, F. Ren, E. Patrick, M. E. Law, and A. Y. Polyakov, ECS J. Solid State Sci. Technol. **5**, Q35–Q60 (2016).
[3]S. Verma, K. C. Praveen, T. Kumar, and D. Kanjilal, IEEE Trans. Device Mater. Reliab. **13**, 98–102 (2013).
[4]S. O. Kucheyev, J. S. Williams, and S. J. Pearton, Mater. Sci. Eng., R **33**, 51–108 (2001).
[5]A. Kumar, A. Hähnel, D. Kanjilal, and R. Singh, Appl. Phys. Lett. **101**, 153508 (2012).
[6]A. Kumar, T. Kumar, A. Hähnel, D. Kanjilal, and R. Singh, Appl. Phys. Lett. **104**, 033507 (2014).
[7]S. Mansouri, P. Marie, C. Dufour, G. Nouet, I. Monnet, and H. Lebius, Nucl. Instrum. Methods Phys. Res., Sect. B **266**, 2814–2818 (2008).
[8]M. Sall, I. Monnet, F. Moisy, C. Grygiel, S. Jublot-Leclerc, S. Della-Negra, M. Toulemonde, and E. Balanzat, J. Mater. Sci. **50**, 5214–5227 (2015).
[9]A. Kumar, D. Kanjilal, V. Kumar, and R. Singh, Radiat. Eff. Defects Solids **166**, 739–742 (2011).
[10]J. F. Ziegler, M. D. Ziegler, and J. P. Biersack, SRIM, Cadence Design Systems, 2008.
[11]A. Polyakov, N. Smirnov, A. Govorkov, S. Pearton, and J. Zavada, J. Appl. Phys. **94**, 3069–3074 (2003).
[12]S. Kucheyev, H. Timmers, J. Zou, J. Williams, C. Jagadish, and G. Li, J. Appl. Phys. **95**, 5360–5365 (2004).
[13]A. Kumar, S. Arafin, M. Amann, and R. Singh, Nanoscale Res. Lett. **8**, 481 (2013).
[14]S. O. Kucheyev, H. Boudinov, J. S. Williams, C. Jagadish, and G. Li, J. Appl. Phys. **91**, 4117 (2002).
[15]S. K. Cheung and N. W. Cheung, Appl. Phys. Lett. **49**, 85–87 (1986).
[16]R. H. W. E. H. Rhoderick, *Metal-Semiconductor Contacts*, 2nd ed. (Clarendon Press, University of Michigan, 1988).
[17]V. Baranwal, S. Kumar, A. C. Pandey, and D. Kanjilal, J. Alloys Compd. **480**, 962–965 (2009).
[18]S. Kumar, Y. S. Katharria, V. Baranwal, Y. Batra, and D. Kanjilal, Appl. Surf. Sci. **254**, 3277–3281 (2008).
[19]A. Kumar, S. Mahajan, S. Vinayak, and R. Singh, Mater. Res. Express **3**, 085901 (2016).
[20]A. I. Titov, P. A. Karasev, and S. O. Kucheyev, Semiconductors **38**, 1179–1186 (2004).
[21]D. C. Look, D. Reynolds, J. W. Hemsky, J. Sizelove, R. Jones, and R. J. Molnar, Phys. Rev. Lett. **79**, 2273 (1997).
[22]J. Neugebauer and C. G. Van de Walle, Phys. Rev. B **50**, 8067 (1994).
[23]C. Coskun, D. C. Look, G. C. Farlow, and J. R. Sizelove, Semicond. Sci. Technol. **19**, 752–754 (2004).
[24]M. Toulemonde, C. Dufour, and E. Paumier, Phys. Rev. B **46**, 14362–14369 (1992).
[25]C. Dufour, A. Audouard, F. Beuneu, J. Dural, J. P. Girard, A. Hairie, M. Levalois, E. Paumier, and M. Toulemonde, J. Phys.: Condens. Matter **5**, 4573 (1993).
[26]A. Meftah, J. M. Costantini, N. Khalfaoui, S. Boudjadar, J. P. Stoquert, F. Studer, and M. Toulemonde, Nucl. Instrum. Methods Phys. Res., Sect. B **237**, 563–574 (2005).
[27]A. Meftah, F. Brisard, J. M. Costantini, E. Dooryhee, M. Hage-Ali, M. Hervieu, J. P. Stoquert, F. Studer, and M. Toulemonde, Phys. Rev. B **49**, 12457–12463 (1994).
[28]Z. G. Wang, C. Dufour, E. Paumier, and M. Toulemonde, J. Phys.: Condens. Matter **6**, 6733 (1994).
[29]D. J. Suntrup, G. Gupta, H. Li, S. Keller, and U. K. Mishra, Appl. Phys. Lett. **105**, 263506 (2014).
[30]O. Madelung, U. Rössler, and M. Schulz, "Gallium nitride (GaN), thermodynamical parameters, vaporization," in *Group IV Elements, IV-IV and III-V Compounds. Part b - Electronic, Transport*, Optical and Other Properties (Springer, Berlin, Heidelberg, 2002), pp. 1–4.
[31]S. Porowski, Mater. Sci. Eng., B **44**, 407–413 (1997).
[32]A. Jeżowski, B. A. Danilchenko, M. Boćkowski, I. Grzegory, S. Krukowski, T. Suski, and T. Paszkiewicz, Solid State Commun. **128**, 69–73 (2003).
[33]E. Sichel and J. Pankove, J. Phys. Chem. Solids **38**, 330 (1977).
[34]M. E. Levinshtein, S. L. Rumyantsev, and M. S. Shur, *Properties of Advanced Semiconductor Materials: GaN, AlN, InN, BN, SiC, SiGe* (John Wiley & Sons, 2001).
[35]C. M. Wang, W. Jiang, W. J. Weber, and L. E. Thomas, J. Mater. Res. **17**, 2945–2952 (2002).
[36]I. Yonenaga, P. D. Brown, and C. Humphreys, "Climb of dislocations in GaAs by irradiation," Mater. Sci. Eng., A **253**, 148–150 (1998).